The rhizoferrin biosynthetic gene in the fungal pathogen *Rhizopus delemar* is a novel member of the NIS gene family

Cassandra S. Carroll[a], Clark L. Grieve[a], Indu Murugathasan[a], Clarissa M. Czekster[b], Huanting Lui[b], James Naismith[b] and Margo M. Moore[a*]

[a]Department of Biological Sciences, Simon Fraser University, Burnaby, Canada V5A 1S6;

[b]Biomedical Sciences Research Complex, University of St. Andrews, Scotland, United Kingdom

***Corresponding author**

Email: mmoore@sfu.ca

Keywords (6): mucormycosis; *Rhizopus delemar*; siderophore biosynthesis; NRPS-independent siderophore (NIS)

Abbreviations: CAS: chrome azurol S; DKA: diabetic ketoacidosis; NIS: NRPS-independent siderophore; NRPS: non-ribosomal peptide synthetase

Abstract

Iron is essential for growth and in low iron environments such as serum many bacteria and fungi secrete ferric iron-chelating molecules called siderophores. All fungi produce hydroxamate siderophores with the exception of Mucorales fungi, which secrete rhizoferrin, a polycarboxylate siderophore,. Here we investigated the biosynthesis of rhizoferrin by the opportunistic human pathogen, *Rhizopus delemar*. We searched the genome of *R. delemar* 99-880 for a homologue of the bacterial NRPS-independent siderophore (NIS) protein, SfnaD that is involved in biosynthesis of staphyloferrin A in *Staphylococcus aureus*. We identified a protein with 22% identity and 37% similarity with SfnaD that contained an N-terminal IucA/IucC family domain, and a C-terminal conserved ferric iron reductase FhuF-like transporter domain. We showed that expression of the putative fungal rhizoferrin synthetase (*rfs*) gene was repressed by iron. The *rfs* gene was heterologously cloned and expressed in *E.coli* and siderophore biosynthesis from citrate and diaminobutane was confirmed using high resolution LC-MS. Substrate specificity was investigated showing that Rfs produced AMP when oxaloacetic acid, tricarballylic acid, ornithine, hydroxylamine, diaminopentane and diaminopropane were employed as substrates. Based on the production of AMP and the presence of a mono-substituted rhizoferrin, we suggest that Rfs is a member of the superfamily of adenylating enzymes. We used site-directed mutagenesis to mutate selected conserved residues in the Rfs active site, chosen based on multiple sequence alignments of NIS genes from bacteria. These studies revealed that H484 is essential for Rfs activity and L544 may play a role in amine recognition by the enzyme. This study on Rfs is the first characterization of a fungal NIS enzyme.

1. Introduction

Mucormycosis is a potentially life-threatening infection in immunocompromised individuals caused by Mucorales fungi. The most commonly-isolated clinical specimens belong to the genera *Rhizopus, Mucor, Cunninghamella* and *Lichtheimia* (Alvarez et al., 2009; Park et al., 2011) though *Rhizopus* species account for up to 70% of mucormycosis infections (Roden et al., 2005). Some species within *Rhizomucor, Saksenaea* and *Apophysomyces* are also pathogenic but are less commonly isolated (Roden et al., 2005). Populations at risk include those with hematological malignancies, particularly acute myeloid leukemia (Pagano et al., 1997), as well as hematopoietic stem cell transplant recipients (HSCT) (Sun and Singh, 2008), patients with uncontrolled diabetes (Roden et al., 2005) or those with elevated serum iron levels (Boelaert et al., 1994; Spellberg et al., 2005). Patients with diabetic ketoacidosis (DKA) have elevated blood glucose levels (Liu et al., 2010) and low blood pH (< 7.3); the lower pH is thought to cause proton-mediated release of iron from transferrin (Artis et al., 1982). This increase in free iron reduces the fungistatic properties of serum allowing for growth and proliferation of *Rhizopus* species (Waldorf et al., 1984). Interestingly, the ability to colonize DKA patients is unique to Mucorales fungi; *Aspergillus* and *Candida* infections are uncommon in this patient group (Liu et al., 2010). Airborne sporangiospores are the infectious particles; therefore, the primary site of infection is typically the respiratory tract, where spore germination occurs (Park et al., 2011). Clinical manifestations of mucormycosis depend on the immune status of the host and the site of infection (Petrikkos et al., 2012; Spellberg et al., 2005). Fungal hyphae may penetrate the epithelial and endothelial barriers of the respiratory tract and disseminate hematogenously (Liu et al., 2010) particularly to the brain. Individuals with iron overload or profound immune-suppression are particularly susceptible to disseminated infection (Roden et al., 2005). Liposomal

amphotericin B and posaconazole are the main antifungal agents used in chemotherapy (Cornely et al., 2014); however, even with treatment, mortality rates can be as high as 70% (Kyvernitakis et al., 2016).

Iron is an essential nutrient for both the host and pathogen as it is required for many biological processes including DNA synthesis and cellular respiration (Haas, 2003). To limit the growth of pathogens in vivo, serum contains iron-binding proteins such as transferrin and lactoferrin that maintain a very low concentration of free iron (~10^{-18} M). To overcome this iron limitation, many bacteria and fungi secrete siderophores, low molecular weight ferric iron chelators (Hissen et al., 2004; Li et al., 2016). Hydroxamate siderophores (named for the moiety that complexes ferric iron) are the major class produced by non-Mucorales fungi. In contrast, fungi within the order Mucorales have been shown to produce the polycarboxylate siderophore rhizoferrin (Drechsel et al., 1991; Thieken and Winkelmann, 1992). Rhizoferrin was first characterized in *Rhizopus microsporus var. rhizopodiformis* (Drechsel et al., 1991) and has since been found to be produced by several species within the Mucorales order (Thieken and Winkelmann, 1992). The chemical structure of rhizoferrin consists of a diaminobutane backbone linked to two citric acid moieties, with an *R,R*- configuration around the chiral center (Figure 1A) (Drechsel et al., 1992). Rhizoferrin is also produced by *Francisella tularensis* and *Ralstonia* (*Pseudomonas*) *pickettii* (Sullivan et al., 2006; Taraz et al., 1999). The two siderophores have the same molecular formula; however, bacterial rhizoferrin is an enantiomer of fungal rhizoferrin with an *S,S* configuration around the chiral center (Sullivan et al., 2006; Taraz et al., 1999). While the structure of *R,R*-rhizoferrin has been elucidated, little is known about its biosynthesis in Mucorales.

The biosynthesis of siderophores is known to occur via two main pathways. The first involves non-ribosomal peptide synthetases (NRPS) that catalyze the condensation of multiple amino acids to form siderophores such as *N,N',N''*-triacetylfusarinine C (Hissen et al., 2005), vibriobactin (Keating et al., 2000), enterobactin (Walsh et al., 1990) and petrobactin (Oves-Costales et al., 2007). The second relies on an NRPS-independent siderophore (NIS) pathway. NIS enzymes function by adenylating a substrate carboxyl group for subsequent condensation with a polyamine or amino alcohol (Gulick, 2009). At present, there are four proposed classes for NIS enzymes based on their substrate specificity for polyamines or amino alcohols and which substrate is activated for downstream condensation (Cotton et al., 2009; Oves-Costales et al., 2009). Type A NIS synthetases catalyze the condensation of citric acid with various amines and alcohols. The Type A' NIS synthetase sub category catalyzes the condensation of citric acid specifically with amines. Type B NIS synthetases are predicted to catalyze the condensation of α-ketoglutarate with amines; however, only one such enzyme has been biochemically characterized (Kadi and Challis, 2009). Type C NIS synthetases are specific for monoamine or monoester derivatives of citric acid, or monohydroxamate derivatives of succinic acid, and some type C NIS synthetases are known to catalyze the formation of oligomeric/macrocyclic siderophores (Oves-Costales et al., 2009).

Cotton et al. (2009) determined that the NIS enzymes, SfnaD and SfnaB are responsible for biosynthesis of the polycarboxylate siderophore, staphyloferrin A (Figure 1B) in the bacterial pathogen, *Staphylococcus aureus*. In *S. aureus,* SfnaD condenses one molecule of citric acid to D-ornithine forming a citryl-ornithine intermediate which is then used as substrate by SfnaB to condense a second molecule of citrate, yielding the final product staphyloferrin A (Cotton et al., 2009).

Unlike staphyloferrin A, rhizoferrin is a symmetric molecule; therefore, we hypothesized that the synthesis of rhizoferrin should require only a single Sfna-like enzyme to catalyze the condensation of two molecules of citrate to one molecule of diaminobutane in sequential reactions. We also hypothesized that the enzymatic mechanism of action was similar to AcsD (Schmelz et al., 2009), the NIS synthetase responsible for biosynthesis of the bacterial carboxylate siderophore achromobactin (Franza et al., 2005; Münzinger et al., 2000). In the AcsD-catalyzed reaction adenylation of citrate is followed by capture of diaminobutane and release of adenosine monophosphate (AMP) and the mono-citryl intermediate from the enzyme active site. This reaction would occur twice during the formation of rhizoferrin.

In this study, we demonstrate the iron-regulated production of rhizoferrin by various pathogenic Mucorales fungi. In *Rhizopus delemar*, we showed that rhizoferrin biosynthesis is catalyzed by rhizoferrin synthetase (Rfs) and that this enzyme is transcriptionally regulated by iron. We confirmed that the preferred substrates of Rfs are diaminobutane and citrate, characteristic of Type A' NIS proteins and confirmed the placement of Rfs in this family of proteins using phylogenetic analysis. Rfs used oxaloacetic acid and tricarballylic acid as carboxylate substrates. Rfs was also capable of using ornithine, hydroxylamine, diaminopropane and diaminopentane as nucleophilic substrate derivatives. Finally, mutagenesis studies revealed critical amino acids in the active site that are required for activity. To our knowledge, our study of Rfs represents the first characterization of a fungal NIS enzyme.

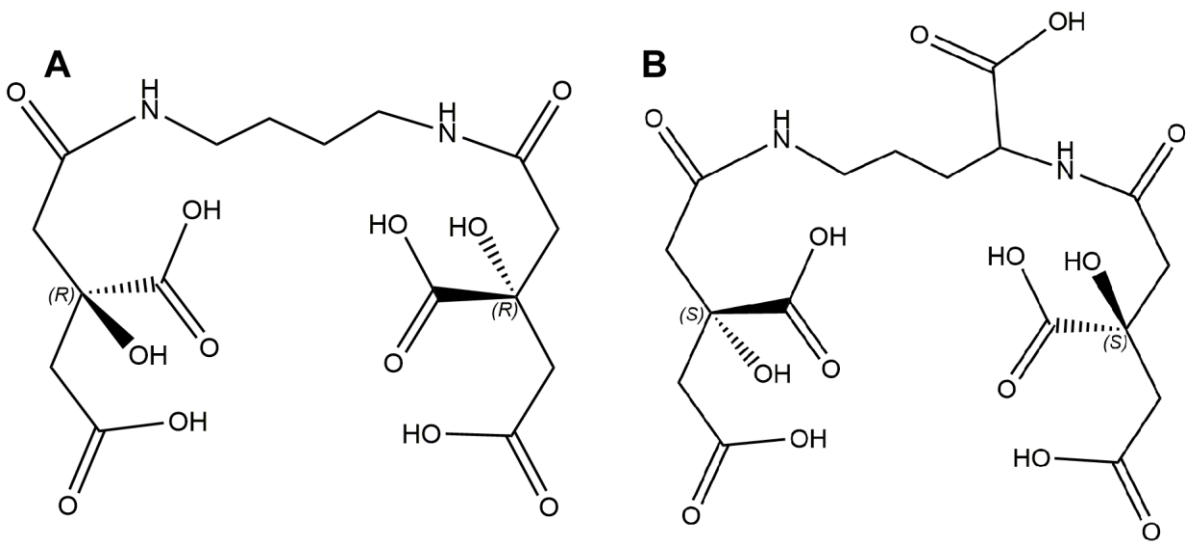

Figure 1. The chemical structures of (A) *R,R*-rhizoferrin and (B) *S,S*-staphyloferrin.

2. Materials and Methods

2.1 Bioinformatic analyses

Bioinformatic analyses were conducted using the genomic sequence of *Rhizopus delemar* (99-880) published by Ibrahim et al., 2009, and acquired from Genbank (accession: PRJNA13066). Genetic information about *rfs* (accession: RO3G_06864) was obtained from NCBI. Conserved domains were identified in the Rfs protein sequence using the NCBI Conserved Domain Database (Marchler-Bauer et al., 2015) and Blastp was used to identify Rfs homologs (Altschul et al., 1990).

Phyre and I-TASSER (A. Roy, A. Kucukural, 2011; Kelley et al., 2015) were used to predict the structure of Rfs using the crystal structure of AcsD as a template (PDB: 2W02). PyMOL was used for structural alignments and to produce all protein structure figures (The PyMOL Molecular Graphics System, Version 1.8 Schrödinger, LLC).

Phylogenetic analyses were carried out on NIS synthetases using a Clustal Omega multiple sequence alignment (Sievers et al., 2011) and the following annotated NIS enzymes from bacteria, RhbC (*Sinorhizobium meliloti*; accession: WP_010968203.1), AcsD (*Dickeya dadantii*; accession: WP_013317292.1), IucA (*Escherichia coli*; accession: AAZ29624.1), PvsD (*Vibrio alginolyticus*; accession: ABM30202.1), AcsC (*Dickeya chrysanthemi*; accession: AAL14570.1), AlcC (*Bordetella spp*.; accession: WP_010926978.1), DesD (*Streptomyces scabiei*; accession: WP_013003384.1), AsbB (*Bacillus cereus*; accession: WP_011053144.1), SfnaD (*Staphylococcus aureus*; accession: WP_001052566.1), SfnaB (*Staphylococcus aureus*; accession: WP_072519492.1), FslA (*Francisella tularensis*; accession: WP_003022888.1) and AsbA (*Bacillus anthracis*; accession: WP_000679659.1). Analysis of the multiple sequence alignment was done using Jalview (version 2.10.1; Waterhouse et al., 2009).

Phylogenetic analyses were completed using Geneious (version 9.1.5; Kearse et al., 2012) and a Neighbor-Joining consensus tree was made using the NIS protein sequences listed above. Bootstrap values are indicated at branch nodes.

2.2 Strains, media and culture conditions

Rhizopus delemar 99-880 was obtained from American Type Culture Collection (ATCC). It was grown on potato dextrose agar (PDA) at 37°C until sporulation. Sporangiospores were harvested and spore stocks were stored at -20°C in phosphate buffered saline (8 g NaCl, 0.2 g KCl, 1.44 g Na_2HPO_4, 0.24 g KH_2PO_4, 1 L water, pH 7.4) amended with 25% glycerol. *Mucor circinelloides* (UAMH 8307), *Lichtheimia corymbifera* (UAMH 10324) and *Rhizomucor pusillus* (UAMH 10076) were obtained from the University of Alberta Microfungus Collection and Herbarium. *Syncephalastrum racemosum*, *Cunninghamella echinulata* and *Mucor heimalis* were obtained

from the culture collection at Simon Fraser University (Burnaby, Canada). To induce siderophore expression, fungi were grown in low iron media, Media A (20 g sucrose, 3 g $(NH_4)_2SO_4$, 1 g K_2HPO_4, 1 g KH_2PO_4, 25 mg $MgSO_4 \bullet 7H_2O$, 10 mg $CaCl_2 \bullet 2H_2O$, 0.2 mg $ZnSO_4 \bullet 7H_2O$, 1 L water) or Eagle's Minimum Essential Medium (MEM; Sigma) + 10% human serum (male AB positive; Sigma). *Escherichia coli* DH5α (F– Φ80*lac*ZΔM15 Δ(*lac*ZYA-*arg*F) U169 *rec*A1 *end*A1 *hsd*R17 (rK–, mK+) *pho*A *sup*E44 λ– *thi*-1 *gyr*A96 *rel*A1) was used in standard cloning procedures. Tuner *E. coli* (F^- lacY ompT gal dcm lon $hsdS_B(r_B^- m_B^-)$ λ(DE3 [lacI lacUV5-T7 gene 1 ind1 sam7 nin5]) was used for protein expression. Both *E. coli* strains were grown on Luria-Bertani (LB) media (10 g tryptone, 10 g NaCl, 5 g yeast extract, 1 L water) supplemented with ampicillin (100 µg/ml) or kanamycin (30 µg/ml) as needed. All transformations were done using heat-shock and *E. coli* cells were made competent via incubation in 100mM $CaCl_2$ or in some cases *E. coli* cells were made ultra-competent (Sambrook and Russell, 2006) for the uptake of small amounts of DNA.

2.3 Rhizoferrin quantification

Total siderophores were quantified using the Chrome Azurol S (CAS) assay. The CAS solution was prepared as previously described (Alexander and Zuberer, 1991). In a 96-well plate, equal volumes of CAS solution and supernatant were mixed together and incubated for 30 minutes at room temperature. Absorbance measurements were taken at 630 nm.

2.4 Rhizoferrin purification from culture media

Rhizoferrin was purified from Media A according to Drechsel et al., 1991. Briefly, fungal sporangiospores were inoculated into Media A (10^5 spores/ml) and incubated overnight at 37°C with shaking at 150 rpm. Mycelia were removed by filtration through Miracloth and the pH of

the clarified culture medium was adjusted to 7.0. This was passed through a Dowex 50WX8 column (formate form) after which the column was washed twice with water. Bound siderophores were eluted with 3M formic acid. The pH of the eluate was adjusted to 7.0 using 10M NaOH and size exclusion chromatography was carried out by applying the eluate to a 5ml column containing Biogel P2 (Bio-Rad Laboratories). One milliliter fractions were collected and CAS-active fractions were pooled and dried by vacuum evaporation.

2.5 Confirmation of rhizoferrin production in pathogenic Mucorales

High pressure liquid chromatography (HPLC) was used to verify the presence of rhizoferrin. Rhizoferrin was purified from cultures as described above and dried or freeze-dried samples were re-constituted in water. Ten microliters were injected into a Gemini C18 column (Phenomenex, 250 x 4.6 mm, 5 µm particle size) and compounds were separated using a gradient of 2% - 40% solvent A over 25 minutes using a flow rate of 1 ml/min. Solvent A consisted of acetonitrile (Fisher Scientific, HPLC grade) plus 0.2% trifluoroacetic acid (Caledon Laboratories). Solvent B was water. Absorbance was monitored at 220 nm. To confirm the presence of rhizoferrin, fractions were collected and mass spectrometry was performed using the Agilent 1200 HPLC and a Bruker maXis Ultra-High Resolution tandem TOF (UHR-Qq-TOF) mass spectrometer. Samples were introduced by flow injection via HPLC with acetonitrile/water (0.1 % formic acid) as mobile phase and spectra were collected under positive electrospray ionization (+ESI).

2.6 Quantification of rhizoferrin production in pathogenic Mucorales

Fungal spores (10^5) were inoculated into MEM containing 10% human serum (male AB positive, Sigma) and incubated at 37°C with shaking. At designated time points, 50 µl aliquots were

removed and stored at -80^{0}C until the CAS assay could be run. Absorbance values were compared to a standard curve constructed using purified rhizoferrin and absolute amounts of siderophore were normalized to fungal dry weights.

2.7 Construction of the pEHISTEV-rfs *vector and* rfs *mutant sequences*

R. delemar spores (10^6) were inoculated into Media A and incubated overnight at 37°C with shaking. Mycelia were harvested and RNA was extracted using the NucleoSpin RNA Plant kit (Macherey-Nagel) and cDNA was synthesized using the iScript cDNA Synthesis Kit (Bio-Rad Laboratories). The putative rhizoferrin synthetase gene *(rfs)* was amplified using the primers BamHI-RfsRev and NotI-RfsFor (Table 1) with added *BamHI* and *NotI* cut sites and cloned into the multiple cloning site of the pEHISTEVa vector (Liu and Naismith, 2009). In this vector, the *rfs* gene was under control of the IPTG inducible promoter and in-frame with a His_6 N-terminal tag. A TEV cleavage site was present for posterior His-tag removal. The resulting vector, pEHISTEV-*rfs* was transformed into competent *E. coli* DH5α and following plasmid purification using the NucleoSpin Plasmid kit (Macherey-Nagel) the cloned *rfs* gene was sequenced (Genewiz, New Jersey, USA) to confirm its fidelity.

Based on the predicted protein structure of Rfs and resides that were found to be crucial for AcsD functioning, we chose to mutate the arginine at position 354 (R354), the histidine at position 484 (H484) and leucine at position 544. R354 and H484 were mutated to alanine residues and L544 was mutated to an arginine. The glutamate at position 209 was mutated to an alanine based on its conservation in characterized NIS synthetases identified in the multiple sequence alignment done in this study.

Site-directed mutagenesis of the *rfs* gene was done using KAPA HiFi Readymix (KAPA Biosystems). The QuikChange Primer Design program (Agilent Technologies) was used to design primers for mutagenesis (Table 1). PCR reactions were carried out according to the manufacturers recommended protocol and products were treated with *DpnI* to digest parental template DNA. Mutant pEHISTEV-*rfs* plasmids were transformed into ultra-competent DH5α *E. coli* cells and selected for by growth on LB containing kanamycin. Successful mutations were confirmed via sequencing (Genewiz, New Jersey, USA).

Table 1. Primers employed in this study. Mutated nucleotides are underlined and recognition sites for restriction endonucleases are in bold.

Primer name	**Primer Sequences (5'— 3')**	**Purpose**
NotI-RfsFor	**GCGGCCGC**TTAGATTGCCTCAGGAACACTTTGAGG	Cloning
BamHI-RfsRev	CT**GGATCC**ATGCCTGTTGCCTCGAGTGAA	Cloning
SDM E209A	TTCTTCTACCATAAAATGGGCACAATCGGTTGTTGAAGGAC GTCCTTCAACAACCGATTGTGCCCATTTTATGGTAGAAGAA	Site directed mutagenesis
SDM_R354A	TTGGGTATCAAAATCTCTTCTGCCCTTGCGACCGTCACACCATTC GAATGGTGTGACGGTCGCAAGGGCAGAAGAGATTTTGATACCCAA	Site directed mutagenesis
SDM_H484A	TATAAACGGTGTCGCATTTGAAGCTGCCGGTCAAAACACATTAG CTAATGTGTTTTGACCGGCAGCTTCAAATGCGACACCGTTTATA	Site directed mutagenesis
SDM L544R	CAGTTTAGAAGAGGTCTTCAAACGCTTATATCACACTTTATTCCACT AGTGGAATAAAGTGTGATATAAGCGTTTGAAGACCTCTTCTAAACTG	Site directed mutagenesis
RFS-RT5'	CTGTAGCACGACCGGATATTT	qPCR
RFS-RT3'	TCCGAAATAGGTGGTGAATGG	qPCR
Act1-RT5'	TGAACAAGAAATGCAAACTGC	qPCR
Act1-RT3'	CAGTAATGACTTGACCATCAGGA	qPCR
FTR1- RT5'	GGTGGTGTCTCCTTGGGTAT	qPCR
FTR1-RT3'	AAGGAAACCGACCAAACAAC	qPCR

Wildtype and mutant pEHISTEV-*rfs* plasmids were purified using the NucleoSpin Plasmid kit (Macherey-Nagel) and transformed into competent Tuner *E. coli* (F– ompT hsdSB (rB– mB–) gal dcm lacY1(DE3)) cells for protein expression.

2.9 O-CAS bioassay for siderophore production

Siderophore secretion by transformed *E. coli* was detected on solid media with a CAS overlay (O-CAS) as described by Perez-Miranda et al., 2007. Briefly, Tuner *E. coli* transformed with the pEHISTEV-*rfs* plasmid were grown overnight at 37°C in liquid LB containing 100µg/ml ampicillin. Five microliters of culture was spotted onto O-CAS media supplemented with 1 mM citric acid and 1 mM diaminobutane, with or without 1mM of the inducer, IPTG. Cultures were incubated for 5 days at room temperature. Positive siderophore secretion was detected by the presence of orange halos around the colonies.

2.10 Expression and purification of Rfs

Rfs was expressed and purified according to Oke et al., 2010 with minor modifications. Briefly, Tuner *E. coli* cultures were incubated until an OD_{600} of 0.8-1.0 and then protein expression was induced with 1 mM IPTG overnight at 16ºC. Cells were pelleted via centrifugation at 1600*g*, the supernatant was removed and cells were lysed using either glass beads (5 µm) or the One Shot cell disruptor (Constant Systems Ltd) in lysis buffer (PBS, 10mM imidazole, 400mM NaCl and1 mg/ml lysozyme). Cellular debris was pelleted by centrifugation at 16,000*g* and the supernatant incubated with Ni-NTA agarose beads (Qiagen) for 1 hour at 4°C. The beads were washed with wash buffer 1 (PBS, 0.4 M NaCl, 20 mM imidazole). Rfs was eluted from the Ni-NTA beads using elution buffer (PBS, 0.4 M NaCl, 250 mM imidazole) and elution fractions were analyzed by SDS-PAGE run at 240V for 20 minutes. Fractions containing Rfs were pooled, dialyzed against 50 mM Tris (pH7.5), 0.4 M NaCl, 1 mM DTT, 0.5 mM EDTA and treated with 1 mg/ml of Tobacco Etch Virus (TEV) protease overnight at 4ºC. TEV protease was purified as previously described (Oke et al., 2010). TEV-cleaved Rfs was dialyzed against 50 mM Tris (pH 7.5), 0.4 M NaCl, 30 mM imidazole and TEV protease was removed via passage over a second

Ni-NTA column. The column was washed with 50 mM Tris (pH 7.5), 0.4 M NaCl, 30 mM imidazole and the column flow through and washes were pooled. This was concentrated using an Amicon Ultra 10K MWCO filter (EMD Millipore), followed by gel filtration with a HiLoad 16/600 Superdex 200 prep grade column (GE Healthcare Life Sciences) using 10 mM Tris (pH 7.5) containing 0.15 M NaCl. One milliliter fractions were collected and proteins analyzed by a 10% SDS-PAGE. Fractions containing protein with the expected molecular mass (72 kDa) were pooled and concentrated using an Amicon Ultra 50K MWCO filter (EMD Millipore). Protein concentrations were determined using the Pierce BCA protein assay kit (ThermoFisher Scientific). Samples were snap frozen in aliquots and stored at -80°C. To confirm protein identity and integrity, an SDS-PAGE was run and the 72 kDa band was excised, digested with trypsin and analyzed via mass spectrometry.

The oligomerization state of Rfs was determined using BlueNative gels as described by (Wittig et al., 2006). Acrylamide gels (4% – 13%) were run for 2 hours at 100 V at 4°C. Rfs (50µg) was run alone or in the presence of 1 mM citric acid and 7 mM diaminobutane or 70 mM DTT. Molecular masses were determined using the NativeMark™ Unstained Protein Standard (Life Technologies, Carlsbad, CA, USA).

2.11 Rfs activity assay

We used a coupled 96-well plate enzyme assay to detect Rfs activity based on the enzymatic production of AMP coupled to lactate dehydrogenase-dependent oxidation of NADH as described by Schmelz et al., 2009b. Rfs activity was monitored using the following conditions: 50mM Tris (pH 8.0), 1mM ATP, 15mM $MgCl_2$, 10mM diaminobutane, 2mM citric acid, 1.5mM phosphoenol pyruvate, 8.4 U pyruvate kinase, 12.6 U lactate dehydrogenase, 4 U myokinase and 5µM Rfs. Samples were incubated at 37°C and NADH oxidation was monitored at 340 nm for

30-60 minutes. Control samples contained either no enzyme or enzyme that had been heat inactivated (98°C for 10 min). Controls adding AMP to the reaction mixture were used to show that the other enzymes used in this assay (pyruvate kinase, lactate dehydrogenase and myokinase) were not limiting the rate of the reaction. To quantify the Rfs activity, a standard curve of NADH was generated over the linear range of 30 – 1000 µM.

2.12 Monitoring the effect of iron on rfs *expression by qPCR*

R. delemar spores were inoculated into Media A and incubated at 37°C with shaking. After overnight incubation, 100µM $FeCl_3$ was added to the cultures at time 0 and the cultures returned to the incubator. At specific times after iron addition, mycelia were harvested by filtration using filter paper and stored in RNAlater (Thermo Fisher Scientific) at 4°C overnight or at -20°C for longer storage. RNA was extracted from mycelia using the NucleoSpin RNA Plant kit (Macherey-Nagel) and the DNase treatment was done in solution followed by the NucleoSpin RNA Plant Clean-up kit (Macherey-Nagel). RNA was quantified using the NanoDrop UV/Vis 2000 spectrophotometer and RNA quality was assessed using agarose gel electrophoresis. RNA (400 ng) was used to synthesize cDNA with the iScript reverse transcription supermix for RT-qPCR kit (Bio-Rad Laboratories). qPCR primers for *rfs* were designed using the Oligo-dT Analyzer and PrimerQuest (Integrated DNA Technologies). Primers for the housekeeping gene actin *(act1),* and the high-affinity iron permease, *ftr1,* were based on Ibrahim et al., 2010 (Table 1). qPCR was performed using the EvaGreen qPCR Mastermix (Applied Biological Materials Inc.) with the following cycling parameters: 95°C for 10 minutes followed by 30 cycles of 95°C for 15 seconds and 60°C for 1 minute. Primer efficiencies for qPCR were comparable for *act1*, *rfs* and *ftr1* gene primers sets (the range was 92 – 98%).

2.13 LC-MS and high resolution mass spectrometry

Lyophilized enzyme reactions were re-suspended in 100 µl dH_2O and separation of rhizoferrin, or its derivatives, was carried out using Phenomenex Luna reverse phase C18 column (100Å, 150mm X 4.6mm). Mobile phase A consisted of 0.1 % trifluoroacetic acid in water while mobile phase B was acetonitrile. A gradient separation using 2 % - 40 % mobile phase A was performed at a flow rate of 1 ml/min. The injection volume was 25 µL and the run was performed at room temperature. For high-resolution mass spectrometry, samples were dissolved in water and injected into an Orbitrap Velos Pro with Dionex Ultimate 3000 HPLC using an Xbridge C18 2.1x100mm column. The mass spectrometry data was acquired in FTMS (Orbitrap) mode from 150-1000m/z from 0-20mins at 30000res in positive ionisation profile mode (ESI+).

2.14 Statistical analyses

Growth experiments and qPCR assays were performed in biological triplicates with three technical replicates. AMP assays were performed with three technical replicates for each condition tested. Data was analyzed using GraphPad Prism software. For qPCR experiments and AMP data, a one-way ANOVA with Tukey's multiple comparison test was used to evaluate significantly different gene expression levels ($P < 0.001$) and enzyme activity. A relative comparison was made for enzyme activity with substrate derivatives only as the linear regression analysis did not yield a random residual plot. Comparisons were made based on the amount of time required to consume half of the NADH present in the assay mixture. All enzyme assays were preformed in technical triplicates.

3. Results

3.1 Rhizoferrin production by species of pathogenic Mucorales

Seven pathogenic Mucorales species including *Rhizopus delemar, Mucor circinelloides, Lichtheimia (Absidia) corymbifera, Syncephalastrum racemosum, Mucor heimalis, Rhizomucor pusillus* and *Cunninghamella echinulata* were grown in iron- limited media (Media A) overnight and rhizoferrin secretion was confirmed in all species using HPLC and mass spectrometry (MS; data not shown); a representative chromatogram and MS spectrum for *R. delemar* is shown in Figure 2. Rhizoferrin elutes with a retention time of 9.0 minutes and the main mass peaks correspond to rhizoferrin – $2H_2O$ + Na^+ (m/z = 423.10) and rhizoferrin – $2H_2O$ (m/z = 401.11). The chrome azurol S (CAS) assay was used to quantify total rhizoferrin secretion into serum-containing medium. Although *Rhizopus delemar* produced the highest amount of rhizoferrin during log phase (data not shown), when normalized to biomass, *Lichtheimia corymbifera* yielded the greatest amount of rhizoferrin (Figure 3). Siderophore concentrations ranged from approximately 7-30 μg/mg dry weight for the 7 species, comparable to levels found in other filamentous fungi (Hissen et al., 2004).

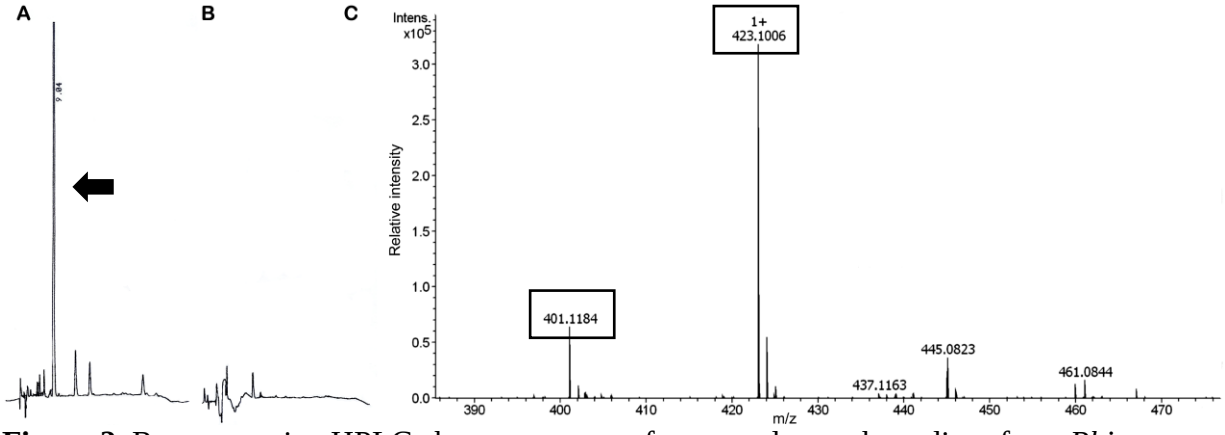

Figure 2. Representative HPLC chromatograms of extracted growth medium from *Rhizopus delemar*. HPLC traces of culture extracts from *R. delemar* grown in (A) low iron medium and (B) iron replete medium. Arrow: the peak corresponding to rhizoferrin at 9.04 minutes. (C) Mass spectrum showing detection of rhizoferrin from the extract from B. The main peak corresponds to rhizoferrin – $2H_2O$ + Na^+ (m/z = 423.10) while the next most abundant peak is rhizoferrin – $2H_2O$ (m/z = 401.11).

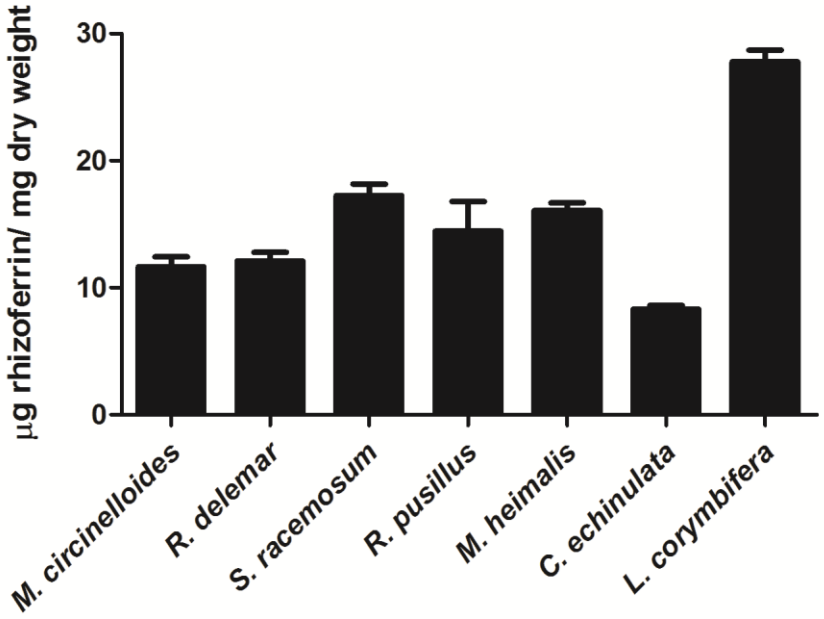

Figure 3. Siderophore production by 7 species of pathogenic Mucorales fungi grown in iron-limited medium. Fungi were inoculated into MEM plus serum and grown at 37°C. Total siderophore content of the culture supernatant was determined during exponential phase (approximately 15 hours) using the CAS assay. The values are normalized to dry biomass yield.

3.2 Bioinformatic analyses

Cotton et al., 2009 reported that the NIS enzymes SfnaD and SfnaB are responsible for the two-step biosynthesis of the polycarboxylate siderophore, staphyloferrin A in *Staphylococcus aureus.* A homologue of SfnaD was identified in *R. delemar* (strain 99-880) with 22% identity and 37% similarity between the putative Rfs protein and SfnaD. The 2.1kb *rfs* gene was predicted to contain 6 exons and 5 introns. The protein was predicted to be cytosolic, have 634 amino acids and contain the conserved N-terminal IucA/IucC family domain, responsible for biosynthesis of the carboxylate siderophore, aerobactin (Neilands, 1992). A C-terminal conserved ferric iron reductase FhuF-like transporter domain was also predicted in the protein. I-Tasser modelling (A. Roy, A. Kucukural, 2011) generated a protein structure alignment with AcsD with 100% confidence. Based on these information, we proposed a biosynthetic pathway for rhizoferrin in

371 which Rfs catalyzes the ATP-dependent condensation of citrate with diaminobutane in the first
372 step followed by the addition of a second citrate to the monocitryl-diaminobutane intermediate
373 (Figure 4).

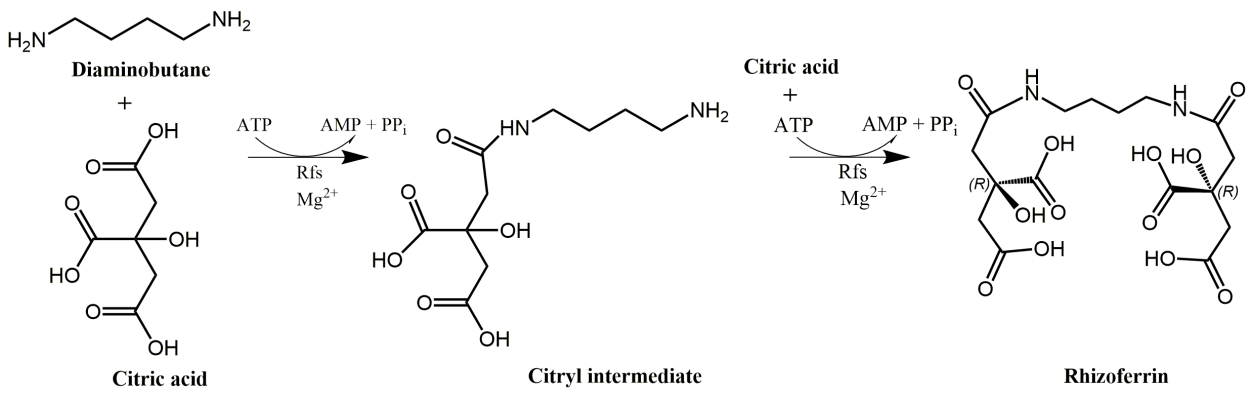

374

375 **Figure 4**. Proposed biosynthetic pathway for fungal rhizoferrin

376 *3.3 Phylogenetic analysis of the putative rhizoferrin synthetase gene of* Rhizopus delemar

377 Phylogenetic analysis of the predicted *rfs* protein resulted in good agreement with Type A' NIS
378 enzymes (Figure 5). These enzymes, including FslA and SfnaD, use citric acid and either
379 diaminobutane or ornithine in the formation of bacterial siderophores *(S,S-)* rhizoferrin and
380 staphyloferrin A, respectively.

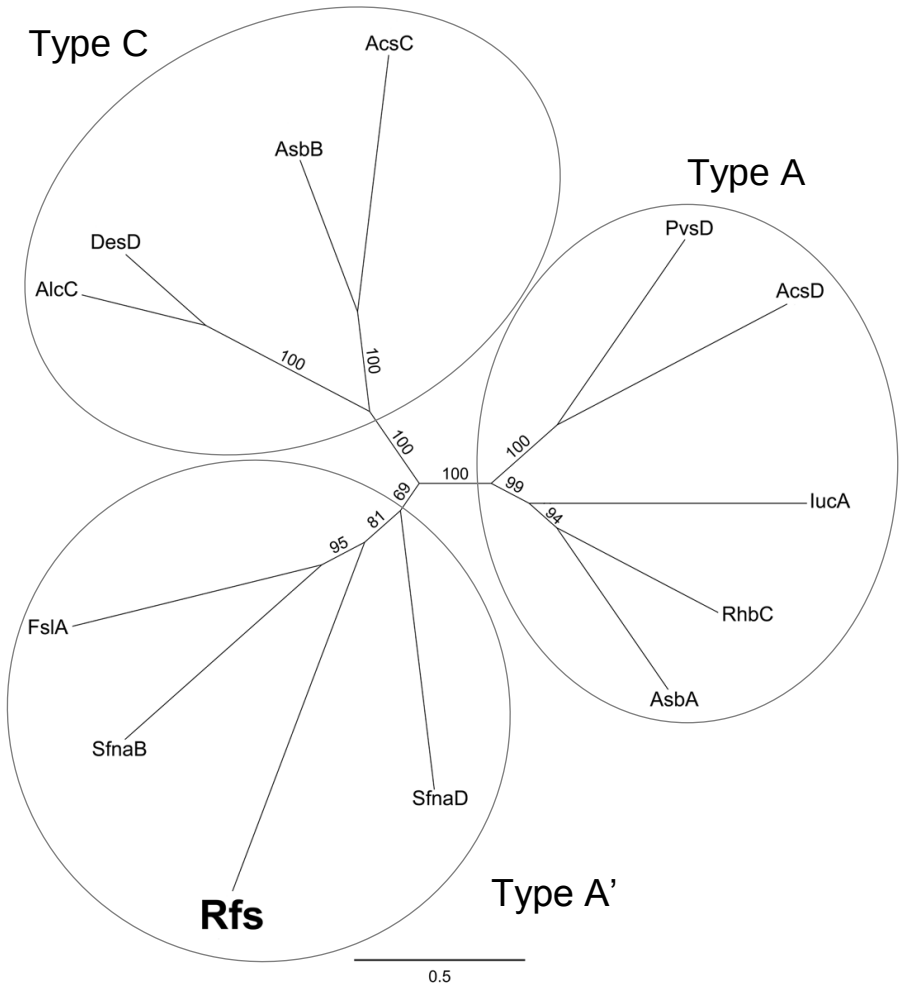

Figure 5. Phylogenetic analysis of *rfs* with bacterial NIS enzymes shows that Rfs (in bold) is a Type A' NIS. The neighbour-joining phylogenetic tree was constructed using Geneious 9.1.5 (Kearse et al., 2012) and bootstrap values are indicated at branch nodes. NIS enzyme sequences used in the tree and the siderophore they biosynthesize are as follows: AsbB and AsbA - Anthrax siderophore biosynthesis (petrobactin); DesD - desferrioxamine biosynthesis; AlcC - alcaligin biosynthesis; FslA – *S, S*-rhizoferrin biosynthesis; SfnaB and SfnaD – staphyloferrin A biosynthesis; RhbC - rhizobactin biosynthesis; IucA – aerobactin biosynthesis; AcsD and AcsC – achromobactin biosynthesis; PvsD – vibrioferrin biosynthesis.

3.5 Regulation of rfs *expression by iron*

To determine whether the putative *rfs* gene expression is regulated by iron, *Rhizopus delemar* was grown overnight in iron-limited medium, washed and transferred to iron-replete medium. Fungal mycelia grown in complete media (MEA) were used as a control. RNA was extracted

from mycelia harvested over time. qPCR analysis confirmed that *rfs* expression was repressed in iron-replete media within 30 minutes and remained at low levels of expression for 3 h post transfer (Table 2). Previous work using Northern blots showed that expression of *ftr1*, the high affinity iron permease gene present in *R. delemar*, is iron-regulated (Ibrahim et al., 2010). Here, qPCR analysis confirmed that *ftr1* expression levels are repressed under iron supplementation. This trend is similar to *rfs* expression levels, confirming the iron-regulated nature of *rfs* expression.

	rfs expression					*ftr1* expression				
Growth condition[a]	*rfs* avg. C_T	*act1* avg. C_T	ΔC_T	$\Delta\Delta C_T$	Fold change in *rfs* expression $(2^{-\Delta\Delta CT})^d$ (range)	*ftr1* avg. C_T	*act1* avg. C_T	ΔC_T	$\Delta\Delta C_T$	Fold change in *ftr1* expression $(2^{-\Delta\Delta CT})^d$ (range)
0 hr	16.09	17.84	-1.75	0.00	1.01 (0.82 – 1.17)	17.08	17.84	-1.45	0.00	1.02 (0.88 – 1.27)
0.5 hr	20.24	17.73	2.51	4.26	0.06 (0.02 – 0.12)	20.80	17.73	1.30	2.75	0.15 (0.13 – 0.18)
1 hr	21.36	18.97	2.39	4.14	0.06 (0.03 – 0.12)	22.28	18.97	3.61	5.06	0.03 (0)
2 hr	20.98	18.58	2.40	4.15	0.06 (0.03 – 0.11)	22.43	18.58	3.38	4.83	0.04 (0.03 – 0.04)
3 hr	21.42	18.29	3.14	4.89	0.04 (0.02 – 0.05)	22.59	18.29	4.07	5.52	0.02 (0.02 – 0.03)
MEA	24.38	22.97	1.41	3.16	0.05 (0.04 – 0.08)	24.11	22.97	3.86	5.31	0.03 (0.02 – 0.03)

Table 2. *rfs* and *ftr1* gene expression in iron limited and iron replete media. *Rhizopus delemar* was grown overnight in Media A and then transferred to iron replete media (low iron media supplemented with 100µM $FeCl_3$) at time 0. Mycelia were harvested at specific times and RNA was extracted. Mycelia grown in complete media (MEA) was used as an iron-replete control. **[a]**Data reported are the mean of independent triplicate runs conducted for each sample of RNA from the different growth conditions, with the exception of *rfs* expression in MEA which was run in duplicate. *act1* was used as the reference gene to normalize data. **[b]**ΔC_T = C_T value of gene of interest - C_T value of *act1*. **[c]**$\Delta\Delta C_T$ = ΔC_T test condition - ΔC_T calibrator condition. The calibrator condition is the zero hour time point. **[d]**Fold change value is calculated as $2^{-\Delta\Delta CT}$.

3.4 Activity of Rfs overexpressed in E. coli

The *rfs* gene was successfully cloned and expressed in Tuner *E. coli* and *E.coli* harbouring the pEHISTEVa-*rfs* plasmid were capable of producing a siderophore from diaminobutane and citric acid. Siderophore production was detected by the presence of orange halos around colonies spotted on O-CAS media (Figure S1). Expression conditions for Rfs in Tuner *E. coli* were optimized, and a 72 kDa protein corresponding to Rfs was purified by nickel affinity chromatography, followed by gel filtration (Figure S2).

The oligomerization state of Rfs was determined using a BlueNative gel, in which the protein complex migrates independent of its charge. Based on the gel, Rfs forms an oligomeric complex in pH 7.5 buffer; however when in pH 8.0 buffer (used in the AMP assay) and in the presence of citric acid and diaminobutane, Rfs adopts a monomer configuration (Figure S3). \

Rhizoferrin biosynthesis by purified Rfs from citrate and diaminobutane was confirmed using high resolution LC-MS (Figure 6). The main peak observed corresponds to rhizoferrin + H^+ (*m/z* = 437.1393) and a peak was also observed for rhizoferrin - H_2O (*m/z* = 419.1296). A peak corresponding to the mono-citryl intermediate was also observed (m/z = 263.1234). This suggests that Rfs forms an adenylated-citryl intermediate that is displaced from the active site upon nucleophilic capture of diaminobutane. These peaks were not present in control reactions prepared using boiled Rfs enzyme (data not shown).

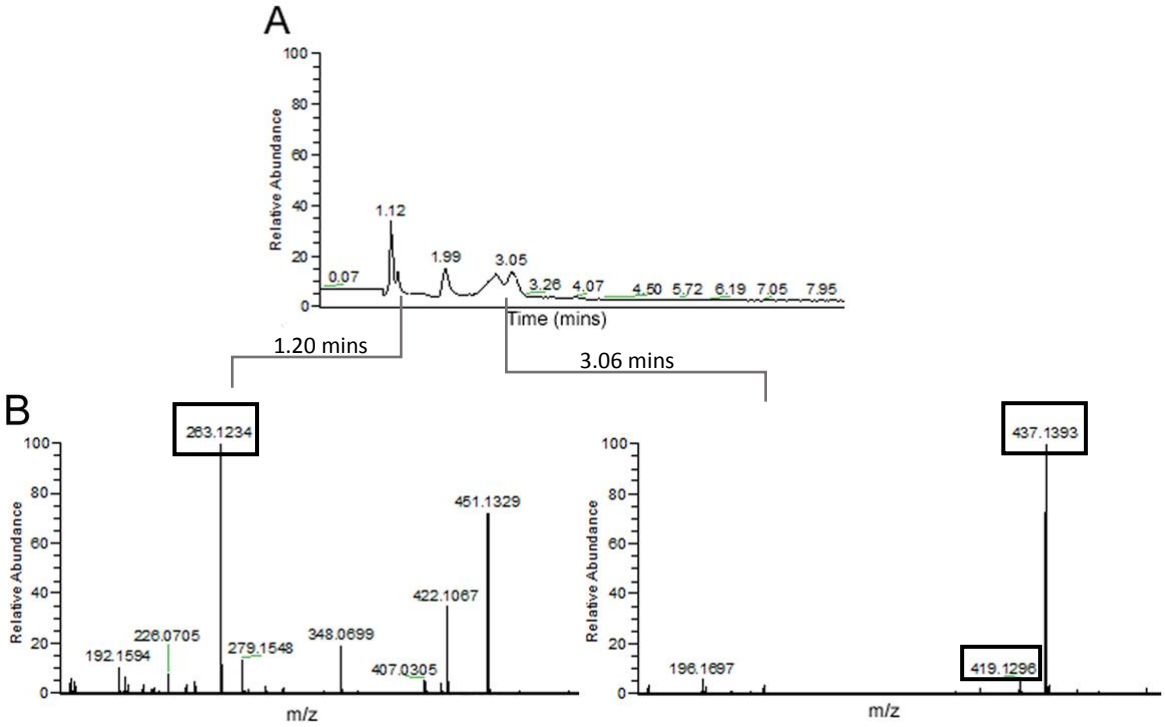

Figure 6. LC-MS/MS confirmation of rhizoferrin biosynthesis in vitro by recombinant Rfs from *R. delemar*. (A) Liquid chromatography trace of the Rfs reaction and (B) the corresponding mass spectra from peaks at 1.20 minutes and 3.06 minutes. Masses corresponding to rhizoferrin are highlighted in boxes. The mono-citryl intermediate of rhizoferrin was found (m/z = 263.1234) as well as the full compound (rhizoferrin + H^+ (*m/z* = 437.1393)). A dehydrated form of rhizoferrin was also present (rhizoferrin - H_2O (*m/z* = 419.1296)).

3.6 Recombinant Rfs kinetic analysis

A coupled AMP production/NADH oxidation assay (Schmelz et al., 2009) was used to monitor Rfs activity. First, we demonstrated that other enzymes used in this coupled enzyme assay, myokinase and lactate dehydrogenase, were not rate limiting; therefore, the rate-limiting step in all reactions was the Rfs catalysis (Figure S4). Kinetic analysis of the fungal NIS showed that Rfs efficiently used diaminobutane and citric acid as substrates. Initial rates for citrate utilization indicated a K_m value of 0.115 ± 0.000 mM, with a V_{max} of 8.91 ± 0.28 µM/min and K_{cat} of 118.7 ± 0.0 sec^{-1}.

446 *3.7 Activity of recombinant Rfs with different substrates*

447 When analyzing substrate derivative data, K_m and V_{max} values could not be determined because
448 linear regression of the NADH consumption versus time data did not produce a random plot of
449 the residuals (data not shown). To circumvent this, we compared the substrate derivatives by
450 measuring the time required for Rfs to consume 50% of the NADH present in the reaction at
451 time 0. Shorter periods of time indicated faster consumption of NADH and therefore, more rapid
452 Rfs activity.

453 The activity of Rfs using the native substrates was compared with equimolar concentrations of
454 various analogues of both citrate and diaminobutane. The following compounds were active in
455 the assay (from highest to lowest activity): oxaloacetic acid, diaminopropane, diaminobutane,
456 diaminopentane, tricarballylic acid, hydroxylamine and ornithine (Figure 7). Negligible activity
457 was detected with butylamine, succininc acid, α-keto glutaric acid, 4-amino-1-butanol and serine.
458 Thus, fungal Rfs was able to use both oxaloacetic acid and tricarballylic acid as citrate
459 analogues. To determine whether Rfs completed the condensation of the analogues, LC-MS/MS
460 was performed on lyophilized enzyme reactions. Rfs formed only a mono-substituted
461 intermediate with oxaloacetic acid and diaminopentane whereas both mono-citryl intermediates
462 and full rhizoferrin derivatives were detected when diaminopropane, and ornithine were used as
463 substrates. Tricarballylic acid only formed a rhizoferrin derivative; no mono-substituted
464 intermediate was detected in this reaction (Table 2).

465

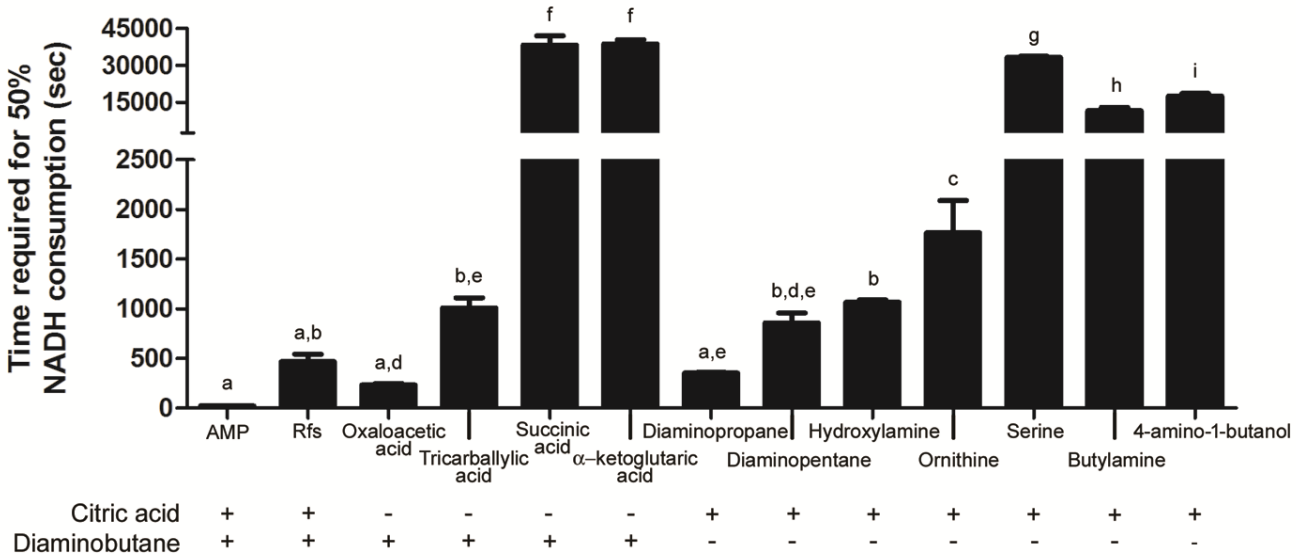

466

467 **Figure 7**. Activity of Rfs using various substrate derivatives. The chemical structure of the tested
468 substrate derivatives is shown above the bar graph. Data is presented as the amount of time
469 required to reach 50% NADH consumption, therefore smaller values indicated faster NADH
470 consumption. The data represent the mean of three measurements and error bars indicate the
471 standard deviation. A one-way ANOVA was used to evaluate significantly different means.
472 Means with the same letter are not significantly different from each other ($P<0.001$).
473

474

Table 2. Expected and actual masses or rhizoferrin derivatives obtained from mass spectroscopy analysis of Rfs reactions. Reactions where no product was observed show only the expected mass in brackets.

	Diaminobutane + Citric acid	**Diaminopentane + Citric acid**	**Diaminopropane + Citric acid**	**Ornithine + Citric acid**	**Oxaloacetic acid + Diaminobutane**	**Tricarballylic acid + Diaminobutane**
	Observed mass (expected mass)	Observed mass (expected mass)	Observed mass (expected mass)	Observed mass (expected mass)	Observed mass (expected mass)	Observed mass (expected mass)
M + H	437.1403 (437.1402)	451.1556 (451.1558)	423.1245 (423.1245)	481.1303 (481.1303)	(317.0979)	405.1504 (405.1503)
M - H_2O + H	(419.1296)	(433.1452)	405.1142 (405.1139)	(463.1197)	(299.0873)	387.1399 (387.1397)
M - citryl + H	263.128 (263.124)	277.1392 (277.1399)	249.1082 (249.1086)	307.1130 (307.1141)	143.0815 (143.082)	(231.1344)

3.8 Site-directed mutagenesis of Rfs

Based on multiple sequence alignments of NIS proteins from bacteria (Figure S6), we used site-directed mutagenesis to mutate selected conserved residues in the Rfs active site (Figure S7). Protein modelling showed that the amino acids chosen for mutation aligned with residues found to be critical in the NIS enzyme, AcsD (Schmelz et al., 2009). Specifically, four mutations were made in Rfs: arginine at position 354 (R354), histidine at position 484 (H484) and glutamate at position 209 (E209) were all mutated to alanine residues, whereas leucine at position 544 was mutated to an arginine (L544R) (Figure S6). R354A and H484A were chosen because these amino acids are predicted to be involved in citrate and ATP recognition in the active site of AcsD. L544R was constructed such that the active site in Rfs mimicked AcsD which is able to use serine (Schmelz et al., 2011). E209 was one of two resides conserved across all NIS enzymes and is located on the periphery of the enzyme active site (Figure S7). However, expression of the E209A protein was poor in multiple bacterial expression hosts under various conditions (data not shown). These data suggest that E209 is a conserved residue that is required for proper folding of Rfs and possibly all NIS enzymes. The R354A mutation did not alter NADH consumption compared to the wild type enzyme (Figure 9). In contrast, H484A was inactive, demonstrating a crucial role in catalysis and/or substrate binding. Using the native substrates diaminobutane and citric acid, L544R had similar activity to the wildtype enzyme. Interestingly, when serine was added in place of diaminobutane, the wild type enzyme had zero activity but L544R was able to accommodate serine in the active site and consumed NADH at a significantly higher rate (Figure 8). This enhanced activity shows that we were successful in expanding the substrate binding pocket of Rfs and may indicate that the residue at position 544 in Rfs plays a role in governing the amino-substrate specificity of NIS enzymes.

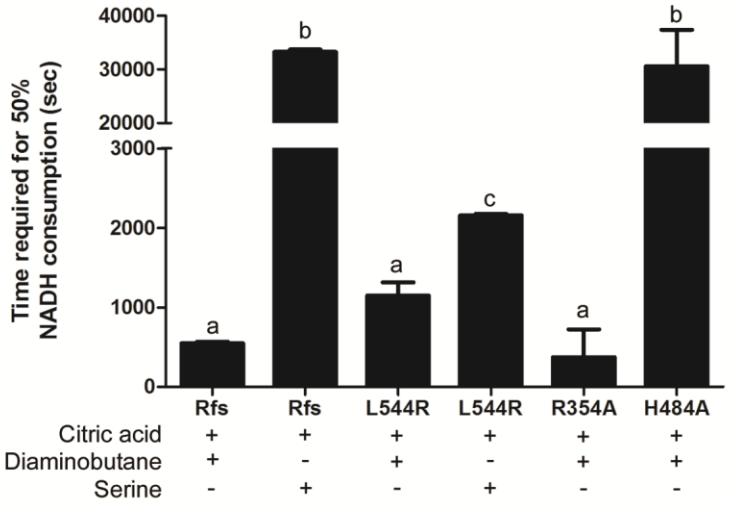

Figure 8. Activity of wild type and mutant Rfs enzymes. Activity of the wild type and Rfs mutants was assessed using the AMP assay with the native substrates, diaminobutane and citric acid, or with serine. H484A displayed very little NADH consumption, while R354A used diaminobutane and citric acid as substrates and consumed NADH at the same rate as the wild type enzyme. L544R can use diaminobutane, citric acid and serine as substrates. The data represent the mean of three measurements and error bars indicate the standard deviation. A one-way ANOVA and Tukey's Multiple Comparison test were used to evaluate significantly different means. Means with the same letter are not significantly different from each other ($P<0.001$).

4. Discussion

This study confirmed and quantified rhizoferrin secretion in seven pathogenic species of Mucorales fungi. While rhizoferrin production has been confirmed in *Mucor mucedo, Rhizopus microsporus var. rhizopodiformis* and *Cunninghamella elegans* (Thieken and Winkelmann, 1992), this is the first confirmation of rhizoferrin production in *Rhizopus delemar, Mucor circinelloides, Lichtheimia (Absidia) corymbifera, Syncephalastrum racemosum, Mucor heimalis, Rhizomucor pusillus* and *Cunninghamella echinulata.* We have also identified and characterized the NIS synthetase responsible for rhizoferrin biosynthesis (Rfs) in the fungal pathogen *Rhizopus delemar*. Of the Mucorales genomes that have been sequenced, Rfs

524 homologues were identified in the following species based on the presence of the conserved
525 IucA/IucC domain (Geer et al., 2002): *L. corymbifera*, *L. ramosa*, *Mucor ambiguus*, *M.*
526 *circinelloides f. lusitanicus*, *M. circinelloides f. circinelloides*, *Rhizopus microsporus*, *Absidia*
527 *glauca*, *Parasitella parasitica*, *Choanephora cucurbitarum* and *Phycomyces blakesleeanus*.
528 Future work will aim to eliminate expression of *rfs* in one of these Mucorales species to
529 determine the role Rfs plays in virulence.

530 The fungal NIS synthetase characterized in this study was shown to be part of the Type A' NIS
531 family and its expression is repressed by iron. Based on the work described here, we proposed a
532 mechanism for rhizoferrin biosynthesis involving ATP-dependent formation of a mono-citryl
533 rhizoferrin intermediate using 1 molecule of citric acid and 1 molecule of diaminobutane (Figure
534 4). The intermediate is then condensed with another molecule of citric acid to form rhizoferrin,
535 using Mg^{2+} as a cofactor and 2 molecules of ATP in total. A similar mechanism has been
536 described for the NIS enzyme, AcsD (Schmelz et al., 2009). In AcsD, adenylation of the
537 carboxylate group in citrate results in an enzyme-bound acyl adenylate intermediate that is
538 condensed with an amine/alcohol resulting in displacement of AMP and the formation of the
539 amide/ester product. AcsD is capable of using a wide range of nucleophilic substrates to
540 synthesize amide and ester derivatives of citric acid via formation of a citryl-adenylate
541 intermediate and AMP, making it a member of the superfamily of adenylating enzymes (Schmelz
542 et al., 2009). Based on their sequence similarity, the production of AMP in the assay and LC-MS
543 detection of the mono-citryl rhizoferrin intermediate, we propose that Rfs is a member of the
544 superfamily of adenylating enzymes and the first fungal member of the NIS family.

545 Rfs is capable of using citric acid derivatives as well as diaminobutane derivatives as substrates.
546 Rfs used oxaloacetic acid and tricarballylic acid as citric acid derivatives and diaminopropane,

diaminopentane, hydroxylamine, and ornithine as diaminobutane derivatives. Interestingly, Rfs was capable of using these derivatives to form di-substituted rhizoferrin derivatives, with the exception of oxaloacetic acid and diaminopentane which formed mono-substituted compounds. In contrast, Tschierske et al. (1996) produced rhizoferrin analogues using directed fermentation with *C. elegans*, and gas chromatography and mass spectrometry confirmed the production of a di-substituted diaminopentane derivative; a derivative using ornithine was not detected and only the mono-substituted tricarballylic acid derivative was found in very low yield. Similar to our study, Tschierske et al. (1996) found that diaminobutane derivatives were more readily incorporated to make rhizoferrin analogues compared to citric acid derivatives. This suggests that citrate recognition in the enzyme active site is stricter compared to the choice of nucleophile.

To investigate the amino acids crucial for Rfs functioning, several mutants were made. Of these mutants, H484A was shown to be essential, most likely involved in ATP binding, as seen in AscD (Schmelz et al., 2009). Additionally, we mutated L544 to an arginine, mimicking the AcsD binding site for serine, a substrate not used by wild type Rfs. We showed that L544R was catalytic active using diaminobutane in the formation of rhizoferrin; however, given the broad range of diaminobutane derivatives which Rfs could accommodate, this was not unexpected. Interestingly, L544R successfully utilized serine as a substrate suggesting that L544 does play a role in nucleophile recognition. Experiments are underway to obtain a crystal structure for Rfs to confirm this hypothesis.

Rhizoferrin secretion has been identified in bacteria, including *Francisella tularensis, Ralstonia pickettii, Morganella morganii* and recently, in *Legionella pneumophila* (Braun et al., 1996; Burnside et al., 2015; Sullivan et al., 2006; Taraz et al., 1999). The molecular formula of rhizoferrin isolated from bacteria and fungi is identical but they are enantiomers: bacterial

rhizoferrin has an *S,S* configuration around the chiral center whereas fungal rhizoferrin has an *R, R* configuration (Drechsel et al., 1992; Taraz et al., 1999). Biosynthesis of bacterial rhizoferrin is catalyzed by the NIS enzyme, FslA in *F. tularensis* (Sullivan et al., 2006) and expression of *fslA* was shown to be iron regulated and transcription occurred as part of an operon (Kiss et al., 2008). This phenomenon was also observed in the biosynthesis of other polycarboxylate siderophores including, staphyloferrin A (Cotton et al., 2009), achromobactin (Berti and Thomas, 2009), vibrioferrin (Tanabe et al., 2003) and petrobactin (Lee et al., 2007). Typically, genes transcribed as part of this operon are involved in secretion of the desferri-siderophore (iron free) or uptake of the ferrated compound. Bioinformatic analyses of the locus surrounding *rfs* in *R. delemar* did not reveal any genes related to metal transport (data not shown). Uptake of ferrated rhizoferrin has been characterized in the bacteria *M. morganii* and *L. pneumophila*. In *L. pneumophila* the inner membrane transporter, LbtB was shown to be involved in export of the desferri-siderophore, while the outer and inner membrane proteins, LbtU and LbtC were shown to mediate ferri-rhizoferrin uptake (Burnside et al., 2015). In *M. morganii*, uptake of ferrated rhizoferrin was shown to occur via the RumA and RumB proteins (Braun et al., 1996). A search of the *R. delemar* proteome did not uncover any homologues (with >16% sequence coverage) to LbtB, LbtU or LbtC. A hypothetical homolog was found for the rumB protein using DELTA-BLAST (Boratyn et al., 2012); the match was weak with 23% coverage and 28% identity for the rumB homologue. The hypothetical *R. delemar* protein (accession: EIE87753.1) contained the TroA_f domain which is indicative of periplasmic binding proteins involved in ABC metal ion uptake in bacteria (Marchler-Bauer et al., 2017). There were no RumA homologues identified in the *R. delemar* proteome. RumA is the outer membrane protein involved in uptake of ferrated

rhizoferrin in *Morganella* species. As a homologue is not present in *R. delemar*, uptake of ferrated-rhizoferrin in Mucorales fungi may occur via a novel mechanism.

This work has successfully identified and characterized the enzyme responsible for rhizoferrin biosynthesis in the pathogenic fungus *Rhizopus delemar*. This may facilitate the development of enzyme inhibitors and such inhibitors may reduce the morbidity and mortality of fungal infections due to *R. delemar*. Future work will aim to determine if rhizoferrin biosynthesis is necessary for virulence of Mucorales fungi.

Acknowledgements

We would like to acknowledge Hongwen Chen (SFU Bruker Spectroscopy Facility, Department of Chemistry, Simon Fraser University) for mass spectrometry services.

Funding

This work was supported by the Natural Sciences and Engineering Research Council of Canada (MM). C. Carroll thanks Simon Fraser University for a travel and research award.

References

A. Roy, A. Kucukural, Y.Z., 2011. I-TASSER: a unified platform for automated protein structure and function prediction. Nat. Protoc. 5, 725–738. doi:10.1038/nprot.2010.5.I-TASSER

Alexander, D.B., Zuberer, D.A., 1991. Use of chrome azurol S reagents to evaluate siderophore production by rhizosphere bacteria. Biol. Fertil. Soils 12, 39–45. doi:10.1007/BF00369386

Altschul, S.F., Gish, W., Miller, W., Myers, E.W., Lipman, D.J., 1990. Basic local alignment search tool. J. Mol. Biol. 215, 403–10. doi:10.1016/S0022-2836(05)80360-2

Alvarez, E., Sutton, D.A., Cano, J., Fothergill, A.W., Stchigel, A., Rinaldi, M.G., Guarro, J., 2009. Spectrum of Zygomycete Species Identified in Clinically Significant Specimens in the United States. Society 47, 1650–1656. doi:10.1128/JCM.00036-09

Artis, W., Fountain, J., Delcher, H., Jones, H., 1982. A Mechanism of Susceptibility to Mucormycosis in Diabetic Ketoacidosis: Transferrin and Iron Availability. Diabetes 31, 1109–1114.

Berti, A.D., Thomas, M.G., 2009. Analysis of achromobactin biosynthesis by Pseudomonas syringae pv. syringae B728a. J. Bacteriol. 191, 4594–4604. doi:10.1128/JB.00457-09

Boelaert, J.R., Van Cutsem, J., de Locht, M., Schneider, Y.J., Crichton, R.R., 1994. Deferoxamine augments growth and pathogenicity of Rhizopus, while hydroxypyridinone chelators have no effect. Kidney Int. 45, 667–71.

Boratyn, G.M., Schäffer, A.A., Agarwala, R., Altschul, S.F., Lipman, D.J., Madden, T.L., 2012. Domain enhanced lookup time accelerated BLAST. Biol. Direct 7, 12. doi:10.1186/1745-6150-7-12

Braun, V., Kuhn, S., Koster, W., 1996. Ferric Rhizoferrin Uptake into Morganella morganii: Characterization of Genes Involved in the Uptake of a Polyhydroxycarboxylate Siderophore. Microbiology 178, 496–504.

Burnside, D.M., Wu, Y., Shafaie, S., Cianciotto, N.P., 2015. The Legionella pneumophila siderophore legiobactin is a polycarboxylate that is identical in structure to rhizoferrin. Infect. Immun. 83, 3937–3945. doi:10.1128/IAI.00808-15

Cornely, O.A., Arikan-Akdagli, S., Dannaoui, E., Groll, A.H., Lagrou, K., Chakrabarti, A., Lanternier, F., Pagano, L., Skiada, A., Akova, M., Arendrup, M.C., Boekhout, T., Chowdhary, A., Cuenca-Estrella, M., Freiberger, T., Guinea, J., Guarro, J., de Hoog, S., Hope, W., Johnson, E., Kathuria, S., Lackner, M., Lass-Flörl, C., Lortholary, O., Meis, J.F., Meletiadis, J., Muñoz, P., Richardson, M., Roilides, E., Tortorano, A.M., Ullmann, A.J., van Diepeningen, A., Verweij, P., Petrikkos, G., 2014. ESCMID and ECMM joint clinical guidelines for the diagnosis and management of mucormycosis 2013. Clin. Microbiol. Infect. 20, 5–26. doi:10.1111/1469-0691.12371

Cotton, J.L., Tao, J., Balibar, C.J., 2009. Identification and characterization of the Staphylococcus aureus gene cluster coding for staphyloferrin A. Biochemistry 48, 1025–35. doi:10.1021/bi801844c

Drechsel, H., Jung, G., Winkelmann, G., 1992. Stereochemical characterization of rhizoferrin and identification of its dehydration products. BioMetals 5, 141–148.

Drechsel, H., Metzger, J., Freund, S., Jung, G., Boelaert, J.R., Winkelmann, G., 1991. Rhizoferrin—a novel siderophore from the fungus Rhizopus microsporus var. rhizopodiformis. BioMetals 4, 238–243.

Franza, T., Mahé, B., Expert, D., 2005. Erwinia chrysanthemi requires a second iron transport route dependent of the siderophore achromobactin for extracellular growth and plant infection. Mol. Microbiol. 55, 261–275. doi:10.1111/j.1365-2958.2004.04383.x

Geer, L.Y., Domrachev, M., Lipman, D.J., Bryant, S.H., 2002. CDART: Protein Homology by Domain Architecture. Genome Res. 12, 1619–1623. doi:10.1101/gr.278202

Gulick, A.M., 2009. Ironing out a new siderophore synthesis strategy. Nat. Chem. Biol. 5, 143–144.

Haas, H., 2003. Molecular genetics of fungal siderophore biosynthesis and uptake: the role of siderophores in iron uptake and storage. Appl. Microbiol. Biotechnol. 62, 316–30. doi:10.1007/s00253-003-1335-2

Hissen, A.H.T., Chow, J.M.T., Pinto, L.J., Moore, M.M., 2004. Survival of Aspergillus fumigatus in Serum Involves Removal of Iron from Transferrin: the Role of Siderophores.

Infect. Immun. 72, 1402–1408. doi:10.1128/IAI.72.3.1402-1408.2004

Hissen, A.H.T., Wan, A.N.C., Warwas, M.L., Pinto, L.J., Moore, M.M., 2005. The Aspergillus fumigatus Siderophore Biosynthetic Gene sidA, Encoding L -Ornithine N 5 -Oxygenase , Is Required for Virulence. Infect. Immun. 73, 5493–5503. doi:10.1128/IAI.73.9.5493

Ibrahim, A.S., Gebremariam, T., Lin, L., Luo, G., Husseiny, M.I., Skory, C.D., Fu, Y., French, S.W., Edwards, J.E., Spellberg, B., 2010. The high affinity iron permease is a key virulence factor required for Rhizopus oryzae pathogenesis. Mol. Microbiol. 77, 587–604. doi:10.1111/j.1365-2958.2010.07234.x

Ibrahim, A.S., Skory, C., Grabherr, M.G., Burger, G., Elias, M., Idnurm, A., Lang, B.F., Sone, T., Abe, A., Calvo, S.E., Corrochano, L.M., Engels, R., Fu, J., Hansberg, W., Kim, J., D, C., Koehrsen, M.J., Liu, B., Miranda-saavedra, D., Ortiz-, L., Shen, Y., Poulter, R., Rodriguez-romero, J., Zeng, Q., Galagan, J., Birren, B.W., Cuomo, C.A., Wickes, B.L., 2009. Genomic Analysis of the Basal Lineage Fungus Rhizopus oryzaeReveals a Whole-Genome Duplication. Genome 5. doi:10.1371/journal.pgen.1000549

Kadi, N., Challis, G.L., 2009. Chapter 17. Siderophore biosynthesis a substrate specificity assay for nonribosomal peptide synthetase-independent siderophore synthetases involving trapping of acyl-adenylate intermediates with hydroxylamine., 1st ed, Methods in enzymology. Elsevier Inc. doi:10.1016/S0076-6879(09)04817-4

Kearse, M., Moir, R., Wilson, A., Stones-Havas, S., Cheung, M., Sturrock, S., Buxton, S., Cooper, A., Markowitz, S., Duran, C., Thierer, T., Ashton, B., Meintjes, P., Drummond, A., 2012. Geneious Basic: an integrated and extendable desktop software platform for the organization and analysis of sequence data. Bioinformatics 28, 1647–9. doi:10.1093/bioinformatics/bts199

Keating, T., Marshall, C., Walsh, C., 2000. Vibriobactin biosynthesis in Vibrio cholerae: VibH is an amide synthase homologous to nonribosomal peptide synthetase condensation domains. Biochemistry 39, 15513–15521. doi:10.1021/bi001651a

Kelley, L.A., Mezulis, S., Yates, C.M., Wass, M.N., Sternberg, M.J.E., 2015. The Phyre2 web portal for protein modeling, prediction and analysis. Nat. Protoc. 10, 845–858. doi:10.1038/nprot.2015.053

Kiss, K., Liu, W., Huntley, J.F., Norgard, M. V., Hansen, E.J., 2008. Characterization of fig operon mutants of Francisella novicida U112. FEMS Microbiol. Lett. 285, 270–277. doi:10.1111/j.1574-6968.2008.01237.x

Kyvernitakis, A., Torres, H.A., Jiang, Y., Chamilos, G., Lewis, R.E., Kontoyiannis, D.P., 2016. Initial use of combination treatment does not impact survival of 106 patients with haematologic malignancies and mucormycosis: a propensity score analysis. Clin. Microbiol. Infect. 22, 811.e1-811.e8. doi:10.1016/j.cmi.2016.03.029

Lee, J.Y., Janes, B.K., Passalacqua, K.D., Pfleger, B.F., Bergman, N.H., Liu, H., Håkansson, K., Somu, R. V., Aldrich, C.C., Cendrowski, S., Hanna, P.C., Sherman, D.H., 2007. Biosynthetic analysis of the petrobactin siderophore pathway from Bacillus anthracis. J. Bacteriol. 189, 1698–1710. doi:10.1128/JB.01526-06

Li, K., Chen, W.-H., Bruner, S.D., 2016. Microbial siderophore-based iron assimilation and

703 therapeutic applications. Biometals 29, 377–388. doi:10.1007/s10534-016-9935-3

704 Liu, H., Naismith, J.H., 2009. A simple and efficient expression and purification system using
705 two newly constructed vectors. Protein Expr. Purif. 63, 102–111.
706 doi:10.1016/j.pep.2008.09.008

707 Liu, M., Spellberg, B., Phan, Q.T., Fu, Y., Fu, Y., Lee, A.S., Jr, J.E.E., Filler, S.G., Ibrahim,
708 A.S., 2010. The endothelial cell receptor GRP78 is required for mucormycosis pathogenesis
709 in diabetic mice. J. Clin. Invest. 120, 1914–1924. doi:10.1172/JCI42164.1914

710 Marchler-Bauer, A., Bo, Y., Han, L., He, J., Lanczycki, C.J., Lu, S., Chitsaz, F., Derbyshire,
711 M.K., Geer, R.C., Gonzales, N.R., Gwadz, M., Hurwitz, D.I., Lu, F., Marchler, G.H., Song,
712 J.S., Thanki, N., Wang, Z., Yamashita, R.A., Zhang, D., Zheng, C., Geer, L.Y., Bryant,
713 S.H., 2017. CDD/SPARCLE: functional classification of proteins via subfamily domain
714 architectures. Nucleic Acids Res. 45, D200–D203. doi:10.1093/nar/gkw1129

715 Marchler-Bauer, A., Derbyshire, M.K., Gonzales, N.R., Lu, S., Chitsaz, F., Geer, L.Y., Geer,
716 R.C., He, J., Gwadz, M., Hurwitz, D.I., Lanczycki, C.J., Lu, F., Marchler, G.H., Song, J.S.,
717 Thanki, N., Wang, Z., Yamashita, R.A., Zhang, D., Zheng, C., Bryant, S.H., 2015. CDD:
718 NCBI's conserved domain database. Nucleic Acids Res. 43, D222–D226.
719 doi:10.1093/nar/gku1221

720 Münzinger, M., Budzikiewicz, H., Expert, D., Enard, C., Meyer, J.M., 2000. Achromobactin, a
721 new citrate siderophore of Erwinia chrysanthemi [WWW Document]. Zeitschrift fur
722 Naturforsch. - Sect. C J. Biosci. URL https://www-ncbi-nlm-nih-
723 gov.proxy.lib.sfu.ca/pubmed?Db=pubmed&Cmd=Retrieve&list_uids=10928541&dopt=abs
724 tractplus (accessed 1.27.17).

725 Neilands, J.B., 1992. Mechanism and regulation of synthesis of aerobactin in Escherichia coli
726 K12 (pColV-K30). Can. J. Microbiol. 38, 728–33.

727 Oke, M., Carter, L.G., Johnson, K. a., Liu, H., McMahon, S. a., Yan, X., Kerou, M., Weikart,
728 N.D., Kadi, N., Sheikh, M.A., Schmelz, S., Dorward, M., Zawadzki, M., Cozens, C.,
729 Falconer, H., Powers, H., Overton, I.M., Van Niekerk, C. a J., Peng, X., Patel, P., Garrett,
730 R. a., Prangishvili, D., Botting, C.H., Coote, P.J., Dryden, D.T.F., Barton, G.J., Schwarz-
731 Linek, U., Challis, G.L., Taylor, G.L., White, M.F., Naismith, J.H., 2010. The Scottish
732 structural proteomics facility: Targets, methods and outputs. J. Struct. Funct. Genomics 11,
733 167–180. doi:10.1007/s10969-010-9090-y

734 Oves-Costales, D., Kadi, N., Challis, G.L., 2009. The long-overlooked enzymology of a
735 nonribosomal peptide synthetase-independent pathway for virulence-conferring siderophore
736 biosynthesis. Chem. Commun. (Camb). 6530–41. doi:10.1039/b913092f

737 Oves-Costales, D., Kadi, N., Fogg, M.J., Song, L., Wilson, K.S., Challis, G.L., 2007. Enzymatic
738 logic of anthrax stealth siderophore biosynthesis: AsbA catalyzes ATP-dependent
739 condensation of citric acid and spermidine. J. Am. Chem. Soc. 129, 8416–8417.
740 doi:10.1021/ja072391o

741 Pagano, L., Ricci, P., Tonso, A., Nosari, A., Cudillo, L., Montillo, M., Corvatta, L., Cenacchi,
742 A., Pacilli, L., Fabbiano, F., Del Favero, A., 1997. Mucormycosis in patients with
743 haematological malignancies : a retrospective clinical study of 37 cases. Br. J. Haematol.

744 99, 331–336.

745 Park, B.J., Pappas, P.G., Wannemuehler, K.A., Alexander, B.D., Anaissie, E.J., Andes, D.R.,
746 Baddley, J.W., Brown, J.M., Brumble, L.M., Freifeld, A.G., Hadley, S., Herwaldt, L., Ito,
747 J.I., Kauffman, C.A., Lyon, G.M., Marr, K.A., Morrison, V.A., Papanicolaou, G., Patterson,
748 T.F., Perl, T.M., Schuster, M.G., Walker, R., Wingard, J.R., Walsh, T.J., Kontoyiannis,
749 D.P., 2011. Invasive non-Aspergillus mold infections in transplant recipients, United States,
750 2001-2006. Emerg. Infect. Dis. 17, 1855–1864. doi:10.3201/eid1710.110087

751 Perez-Miranda, S., Cabirol, N., George-Tellez, R., Zamudio-Rivera, L., Fernandez, F., 2007. O-
752 CAS, a fast and universal method for siderophore detection. J. Microbiol. Methods 70, 127–
753 131. doi:10.1016/j.mimet.2007.03.023

754 Petrikkos, G., Skiada, A., Lortholary, O., Roilides, E., Walsh, T.J., Kontoyiannis, D.P., 2012.
755 Epidemiology and clinical manifestations of mucormycosis. Clin. Infect. Dis. 54 Suppl 1,
756 S23-34. doi:10.1093/cid/cir866

757 Roden, M.M., Zaoutis, T.E., Buchanan, W.L., Knudsen, T. a, Sarkisova, T. a, Schaufele, R.L.,
758 Sein, M., Sein, T., Chiou, C.C., Chu, J.H., Kontoyiannis, D.P., Walsh, T.J., 2005.
759 Epidemiology and outcome of zygomycosis: a review of 929 reported cases. Clin. Infect.
760 Dis. 41, 634–53. doi:10.1086/432579

761 Sambrook, J., Russell, D.W., 2006. The Inoue Method for Preparation and Transformation of
762 Competent E. Coli: "Ultra-Competent" Cells. Cold Spring Harb. Protoc. 2006,
763 pdb.prot3944-prot3944. doi:10.1101/pdb.prot3944

764 Schmelz, S., Botting, C.H., Song, L., Kadi, N.F., Challis, G.L., Naismith, J.H., 2011. Structural
765 basis for Acyl acceptor specificity in the achromobactin biosynthetic enzyme AcsD. J. Mol.
766 Biol. 412, 495–504. doi:10.1016/j.jmb.2011.07.059

767 Schmelz, S., Kadi, N., McMahon, S.A., Song, L., Oves-Costales, D., Oke, M., Liu, H., Johnson,
768 K.A., Carter, L.G., Botting, C.H., White, M.F., Challis, G.L., Naismith, J.H., 2009. AcsD
769 catalyzes enantioselective citrate desymmetrization in siderophore biosynthesis. Nat. Chem.
770 Biol. 5, 174–82. doi:10.1038/nchembio.145

771 Sievers, F., Wilm, A., Dineen, D., Gibson, T.J., Karplus, K., Li, W., Lopez, R., McWilliam, H.,
772 Remmert, M., Söding, J., Thompson, J.D., Higgins, D.G., 2011. Fast, scalable generation of
773 high-quality protein multiple sequence alignments using Clustal Omega. Mol. Syst. Biol. 7,
774 539. doi:10.1038/msb.2011.75

775 Spellberg, B., Jr, J.E., Ibrahim, A., Edwards, J., 2005. Novel Perspectives on Mucormycosis :
776 Pathophysiology , Presentation , and Management. Clin. Microbiol. Rev. 18, 556–569.
777 doi:10.1128/CMR.18.3.556

778 Sullivan, J.T., Jeffery, E.F., Shannon, J.D., Ramakrishnan, G., 2006. Characterization of the
779 siderophore of Francisella tularensis and role of fslA in siderophore production. J. Bacteriol.
780 188, 3785–95. doi:10.1128/JB.00027-06

781 Sun, H.Y., Singh, N., 2008. Emerging importance of infections due to zygomycetes in organ
782 transplant recipients. Int. J. Antimicrob. Agents 32, 115–118.

783 Tanabe, T., Funahashi, T., Nakao, H., Miyoshi, S., Shinoda, S., Yamamoto, S., 2003.

Identification and Characterization of Genes Required for Biosynthesis and Transport of the Siderophore Vibrioferrin in Vibrio parahaemolyticus Identification and Characterization of Genes Required for Biosynthesis and Transport of the Siderophore Vibriof. Society 185, 6938–6949. doi:10.1128/JB.185.23.6938

Taraz, K., Munzinger, M., Budzikiewicz, H., Heymann, P., Winkelmann, G., Drechsel, H., Meyer, J., 1999. S, S-rhizoferrin (enantio-rhizoferrin) – a siderophore of Ralstonia (Pseudomonas) pickettii DSM 6297 – the optical antipode of R, R-rhizoferrin isolated from fungi. Biometals 12, 189–193.

Thieken, A., Winkelmann, G., 1992. Rhizoferrin: A complexone type siderophore of the mocorales and entomophthorales (Zygomycetes). FEMS Microbiol. Lett. 94, 37–41.

Tschierske, M., Drechsel, H., Jung, G., Zahner, H., 1996. Production of rhizoferrin and new analogues obtained by directed fermentation. Appl. Microbiol. Biotechnol. 45, 664–670.

Waldorf, A.R., Ruderman, N., Diamond, R.D., 1984. Specific Susceptibility to Mucormycosis in Murine Diabetes and Bronchoalveolar Macrophage Defense against Rhizopus. J. Clin. Invest. 74, 150–160.

Walsh, C.T., Liu, J., Rusnak, F., Sakaitani, M., 1990. Molecular studies on enzymes in chorismate metabolism and the enterobactin biosynthetic pathway. Chem. Rev. 90, 1105–1129. doi:10.1021/cr00105a003

Waterhouse, A.M., Procter, J.B., Martin, D.M.A., Clamp, M., Barton, G.J., 2009. Jalview Version 2--a multiple sequence alignment editor and analysis workbench. Bioinformatics 25, 1189–1191. doi:10.1093/bioinformatics/btp033

Wittig, I., Braun, H.-P., Schägger, H., 2006. Blue native PAGE. Nat. Protoc. 1, 418–428. doi:10.1038/nprot.2006.62